Three-dimensional numerical simulation of the hydrodynamics generated by a weak breaking tidal bore

B. Simon[1-2], P. Lubin[1], S. Glockner[1] and H. Chanson[2]
[1] Université de Bordeaux, I2M
16, avenue Pey-Berland, CNRS UMR 5295, 33607 PESSAC Cedex
FRANCE
[2] The University of Queensland, School of Civil Engineering
Brisbane St Lucia, QLD 4072
AUSTRALIA
E-mail: bsimon@enscbp.fr

Abstract: *A tidal bore is a positive surge propagating upstream as the tidal flow turns to rising in river mouths exhibiting a converging funnelled channel forms during low freshwater conditions. While some recent laboratory experiments brought new insights to the turbulent motion generated by tidal bores, a numerical model based upon the Navier-Stokes equations is proposed to investigate the complicated features of the flow. The goal of the present work is to simulate this three-dimensional unsteady two-phase tidal bore motion. Therefore, we use a Synthetic Eddy Method to generate the turbulence and a Large Eddy Simulation method to gain a further understanding of the tidal bore processes. The numerical data are compared with some detailed laboratory data and the results are discussed. We aim at describing accurately the free-surface behaviour and the turbulent flow structure. This work is the first attempt to describe this complicated flow with three-dimensional numerical simulation.*

Keywords: *Tidal bore, turbulence, large eddy simulation, three-dimensional modelling, synthetic eddy method.*

1. INTRODUCTION

A tidal bore is a positive surge propagating upstream as the tidal flow turns to rising. It forms during spring tide conditions in river mouth exhibiting a converging funnelled channel form during low fresh water conditions. This natural, powerful and fascinating phenomenon attracts many people eager to watch it and even to surf it. The tidal bore plays an important role in the life of the river. It enhances the turbulent mixing and dispersion because significant bed erosion and scour take place beneath the bore. Meanwhile suspended materials are carried upstream with the tidal bore (Chanson, 2009).

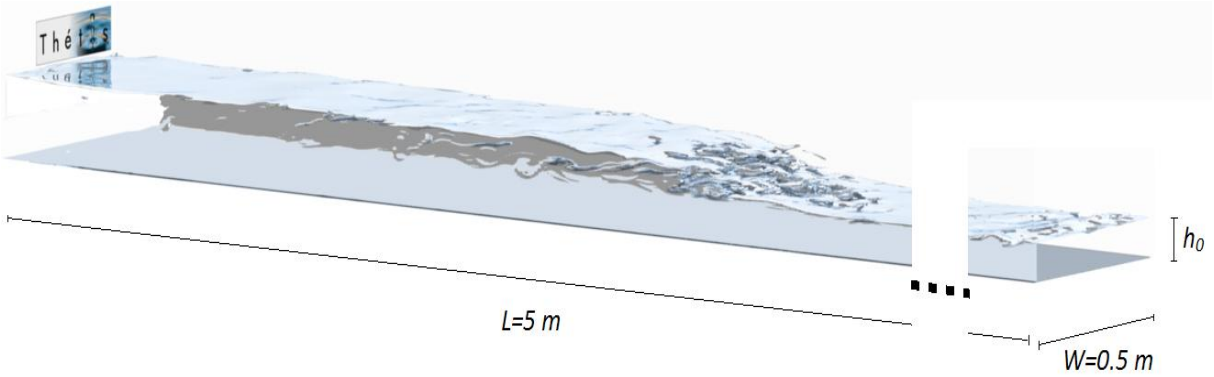

Figure 1 Propagation of the numerical tidal bore.

A recent numerical model based upon the Navier-Stokes equations (Furuyama & Chanson, 2010) was compared to similar laboratory experiments (Koch & Chanson, 2009) with interesting features observed, but the results lacked a fine mesh grid resolution and an accurate numerical scheme. The present study is an extension of the previous work done on the two-dimensional simulation of the tidal bore (Lubin *et al*, 2010a, 2010b), which proved the needs for some realistic unsteady inflow conditions to be specified at the inlet boundary. This work investigates the three-dimensional processes involved

during the unsteady two-phase tidal bore motion (Figure 1) using a Large Eddy Simulation (LES) method to gain a further understanding of the basic mechanisms. Moreover, we aim at describing the effects of the turbulence on the generation of the bore. A new method for inflow condition, the Synthetic Eddy Method (SEM), was implemented to give a more realistic description of the unsteady flow. Some laboratory data (Koch & Chanson, 2005) were used to generate the initial and boundary conditions for the numerical simulation and to validate the numerical results.

2. NUMERICAL MODEL

We solve the Navier-Stokes equations in air and water coupled with a subgrid scale turbulence model (LES). The numerical tool is well suited to deal with strong interface deformations occurring during wave breaking, and more generally with turbulence modelling in the presence of a free surface.

2.1. Governing equations

The Navier-Stokes equations in their multiphase form may describe an incompressible multiphase flow between non-miscible fluids. In the single fluid formulation of the problem, a phase function *C* or "colour" function is normally used to locate the different fluids standing *C=0* in the air and *C=1* in the water. In practice, *C=0.5* is used to characterize the interface between the fluids. The governing equations for the LES of an incompressible fluid flow are derived by applying a convolution filter to the unsteady Navier-Stokes equations. The resulting set of equations reads:

$$\begin{aligned} \nabla \cdot \mathbf{u} &= 0 \\ \rho\left(\frac{\partial \mathbf{u}}{\partial t} + \mathbf{u} \cdot \nabla \mathbf{u}\right) &= -\nabla p + \rho \mathbf{g} + \nabla \cdot \left(\mu + \mu_t\right)\left[\nabla \mathbf{u} + \nabla^T \mathbf{u}\right] \\ \frac{\partial C}{\partial t} + \mathbf{u} \cdot \nabla C &= 0 \end{aligned} \tag{1}$$

where ***u*** is the velocity, *C* the phase function, *t* the time, *p* the pressure, ***g*** the gravity vector, ρ the density, μ the dynamic viscosity and μ_t the turbulent viscosity. The magnitude of the physical characteristics of the fluids is defined in terms of *C* in a continuous manner:

$$\begin{aligned} \rho &= C\rho_1 + (1-C)\rho_0 \\ \mu &= C\mu_1 + (1-C)\mu_0 \end{aligned} \tag{2}$$

where ρ_0, ρ_1, μ_0, and μ_1 are the respective densities and viscosities of fluid *0* and *1*. The turbulent viscosity is calculated with the Mixed Scale model (Sagaut, 2001), which proved its accuracy for geophysical flows (Lubin *et al*, 2006, 2010a, 2010b). The equations (1) and (2) describe the hydrodynamics involved in the motion of multiphase media.

2.2. Boundary conditions

Realistic unsteady inflow conditions are specified at the inlet, i.e. the channel upstream. Some numerical simulations were tested by generating turbulent inflow data consisting of the time-averaged experimental velocity profile with some superimposed random fluctuations. The generated data exhibit neither spatial, nor temporal correlations, and dissipate quickly the pseudo turbulence. An effective method to generate synthetic eddies on the inlet plane was implemented (Jarrin *et al*, 2006). The Large Eddy Simulation of spatially developing flows, such as open-channel flows, requires the specification of instantaneous turbulent inlet fluctuations and these fluctuations depend on the nature of the upstream flow. The SEM generates explicitly large-scale coherent structures and convects them with the mean flow through the inlet plane (Jarrin *et al*, 2006). This method is based upon the approach of considering turbulence as a superposition of coherent structures. These eddies are generated over the inlet plane of our calculation domain and defined by a shape function that

encompasses the spatial and temporal characteristics of the structures. The method generates a stochastic signal with prescribed mean velocity, Reynolds stresses, length and time scale distributions. The number of eddies is a fixed parameter chosen before running the simulation. Although the SEM involves the summation of a large number of eddies for each grid point on the inflow, the CPU time required to generate the inflow data at each iteration is negligible (Jarrin *et al*, 2006). The method performs well on any geometry and any kind of flow (Jarrin *et al*, 2006). We thus implemented and used this method for the generation of the turbulent boundary conditions.

2.3. Numerical methods

Time discretisation is implicit and the equations are discretised on a staggered grid with a finite volume method. A dual grid, or underlying grid, is used to gain an improved accuracy for the interface description, the mesh grid size being divided by two in each direction for the interface tracking. This technique allows avoiding the interpolations of the physical characteristics on the staggered grids, since the colour function C is defined on each point where viscosities and densities are needed. The velocity / pressure coupling is solved with a pressure correction method, which consists in splitting the Navier-Stokes system into two stages, a velocity prediction and a pressure correction. The viscous term is approximated by a second order centered scheme. Interface tracking is achieved by a Volume Of Fluid method (VOF): i.e. a Lax-Wendroff TVD scheme (Total Variation Diminishing) which is able to handle interface reconnections without interface reconstruction. This method is used to solve directly the free-surface evolutions. The MPI library is used to parallelize the code. Numerous test cases including mesh refinement analysis allowed to verify and validate the numerical code. The literature proves the accuracy of the numerical schemes and the conservation laws of mass and energy in the computational domain. For more details on the numerical methods see Lubin *et al* (2010a, 2010b).

3. DESCRIPTION OF THE CASE STUDY

The experimental configuration was the generation of a weak positive surge by a rapid partial gate closure at the downstream end of the control volume and its upstream propagation against the initially steady flow (Koch & Chanson, 2005, 2009). The experimental channel was *0.5 m* wide and *12 m* long, made of smooth PVC bed and glass walls. Detailed velocity and free surface elevation measurements were performed with an acoustic Doppler velocimeter (ADV) located at a distance *5 m* downstream the channel intake and x=*6.15 m* upstream of the fast-closing tainter gate, on the channel centreline. An acoustic displacement meter sampled the free-surface elevation immediately above the ADV sampling volume. However, in order to save CPU time, the numerical domain was selected as *5 m* long; the experimental data were used to feed the inflow boundary condition using the SEM method (section 2.2). Koch and Chanson (2005, 2009) pointed out that the tidal bores are sensitive to the turbulent characteristics of the incoming flow. Hence, the first step of our numerical study was to verify that the numerical tool reproduced the flow correctly prior to the tidal bore generation. The initial conditions of the open-channel flow case study were those used in the three-dimensional Large Eddy Simulation of the weak breaking tidal bore.

The numerical configuration consisted of an initial rectangular steady flow motion (from the right side of the numerical domain to the left side) with an initial steady velocity, impacting a wall boundary located on the left side of the numerical domain. The three-dimensional numerical domain (Figure 1) was *5 m* long, *1 m* high and *0.5 m* wide. The water flowing from the right to the left was set with an initial steady velocity (V_0=*1.021 m.s*$^{-1}$). The initial water depth was h_0=d_0=*0.0785 m*. A no-slip condition was imposed at the lower and lateral boundaries and an open boundary condition was used at the top of the numerical domain. At the left boundary (i.e. downstream end with a fast-closing tainter gate), an open condition was used for the steady-flow and an outlet velocity condition (V_{out}≈*1.764 m.s*$^{-1}$) was fixed for the bore simulation, to let the water flow outside the numerical domain, the outlet height being h_{out}=*0.02 m*. The time step was selected to ensure a CFL number less than *0.1*. The calculation was made with the densities and the viscosities of air and water (ρ_a=*1.1768 kg.m*$^{-3}$ and ρ_w=*1000 kg.m*$^{-3}$, μ_a=*1.85*×*10*$^{-5}$ *kg.m*$^{-1}$*.s*$^{-1}$ and μ_w=*10*$^{-3}$ *kg.m*$^{-1}$*.s*$^{-1}$). The hydrostatic pressure distributions were initialised in the rectangle of water. The numerical domain, discretised into *500*×*500*×*20* regular Cartesian cells, was partitioned into *512* subdomains (one processor per subdomain).
The inlet velocity was calculated at the right side (i.e. upstream end) of the numerical domain at the inlet height d_0=*0.0785 m* using the SEM method. Koch and Chanson (2005) reported that the flow was

not fully developed in the first half of the channel. At *x=6.15 m* from the left gate, the boundary layer thickness was estimated as $\delta/d_0=0.6$ to *0.8*. The velocity distribution followed:

$$\frac{V}{V_{\max}}=\begin{cases}\left(\frac{z}{\delta}\right)^{\frac{1}{N}}, & z\in[0,\delta]\\ 1, & z\in[\delta,d_0]\end{cases} \tag{3}$$

where δ was the boundary layer thickness, z/d_0 was the relative distance to the bed, V was the streamwise velocity component, V_{max} was the free-stream velocity and the exponent N was a function of the bed roughness. In our case, a smooth turbulent flow was considered, which gives $N=7$. The free stream velocity was given by Koch and Chanson (2009, 2005):

$$\frac{V_{\max}}{V_0}=\left(1-\frac{\frac{\delta}{d_0}}{N+1}\right)^{-1} \tag{4}$$

We used the following universal functions of turbulence intensities *u', v'* and *w'* proposed by Nezu (1977, 2005) based on a simplified *k-ε* model and self-similarity theory:

$$\left.\begin{aligned}\frac{u'}{V_*}&=D_u\exp(-C_k\xi)K_u\\ \frac{v'}{V_*}&=D_v\exp(-C_k\xi)K_v\\ \frac{w'}{V_*}&=D_w\exp(-C_k\xi)K_w\end{aligned}\right\}\text{for } 0.1\le\frac{z}{d_0}\le 0.9 \tag{5}$$

where the empirical constants $D_u=2.26$, $D_v=1.27$, $D_w=1.63$ and $C_k=0.88$ are independent of either the Reynolds number or the Froude number. $\xi=z/d_0$ was the relative distance to the bed and $V_*=0.044\ m.s^{-1}$ was the shear velocity measured on the channel centreline (Koch & Chanson, 2005, 2009), used as a velocity scale. V_x, V_y and V_z represent the longitudinal upstream velocity, the transversal velocity and the vertical velocity. The constant $K_u=0.85$, $K_v=0.5$ and $K_w=0.6$ were used to fit the fluctuations recorded in the experimental channel.

4. RESULTS AND DISCUSSION

The numerical data first consisted in running the simulation for a certain time to ensure the establishment of the flow and the turbulence, considering the open channel flow with a Neumann boundary condition specified at the outlet boundary condition. After *14.77 s* of physical time simulation, a wall instantaneously appeared closing partially the channel outlet. When the flow hit the wall, the water ran up the wall and splashed down generating and propagating upstream a weak breaking bore towards the right side of the numerical domain. In both numerical and experimental data *x=0 m* corresponds to the left boundary of the domain, i.e. the gate. The time *t=0 s* corresponds to the closing of the gate. The data are recorded at *y=0.25 m* corresponding to the channel centreline.

Our presentation and discussion of the qualitative comparisons of the numerical and experimental results for the free surface and flow structure demonstrate the efficiency of the numerical tool. They also highlight the limitations of the numerical configuration.

4.1. Free surface results

Figure 2 (A) and (B) show the elevation of the free surface at different locations on the longitudinal

axis from respectively numerical and experimental data (Koch & Chanson, 2005). The time *t=0 s* corresponds for both figures at the gate closure located at *x=0 m*. The numerical and physical data are in close agreement. The sudden elevation of the water surface due to the passage of the bore is similar to the experimental data. The elevation of the water level is about *0.08 m* in both experimental *x=3.9 m* and numerical results *x=3 m*. Numerically the most favourable comparison should be found at *x=4 m*, the data being plotted with the "++" symbols. However, the proximity of the inflow boundary condition disturbs the free surface and imposes us to look at others locations. The same slight elevation prior to the surge is observed at the roller toe. The breaking and splashing of the water diffused the phase function, which explains the oscillation during the surge. In the experimental set up, the water level slowly increases with time after the bore passage. This behaviour is absent because of the short numerical domain configuration as shown in the two-dimensional study (Lubin *et al*, 2010b). The numerical results prove to be very satisfactory.

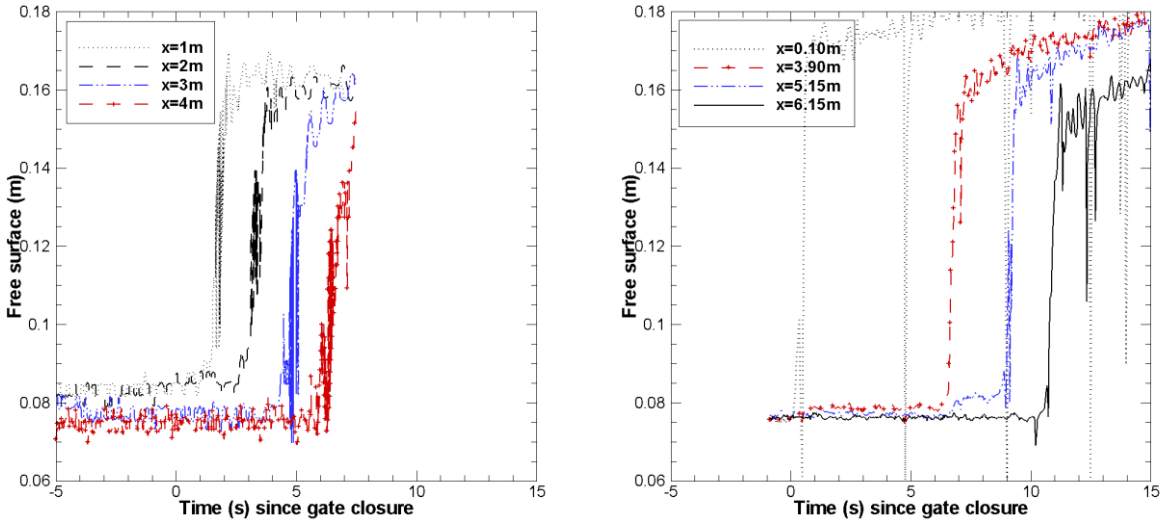

(A) Numerical data (B) Experimental data Koch & Chanson (2005)

Figure 2 Free surface elevation recorded at different longitudinal locations.

4.2. Velocity results

Figure 3 (A) and (B) illustrate the numerical and experimental velocities recorded for respectively *x=2 m* and *x=6.15 m* at three different heights. Note the difference in the position of the numerical and experimental probes. The position *x=2 m* was chosen in order to present significant data after the bore since the simulation ended a few second after the surge. This limitation implies that the comparisons can only be of a qualitative nature. The horizontal velocity is positive in the downstream direction (from right to left, Figure 1). The numerical data show the same rapid deceleration at all vertical elevations during the bore front passage. A small inversion of the velocity signal is also occurring at *z=0.007 m*, near the bed. The amplitude of the deceleration is almost the same in both set of data, about *0.6* to *0.8 m.s*$^{-1}$. As expected the velocity gently decreases as the free surface slightly increases at the roller toe following Koch and Chanson (2005). However several significant differences occurred. Before the bore, the numerical velocity close to the bottom was higher than experimental data, and close to the free surface, it was too low, which accounts for the discrepancies after the bore.

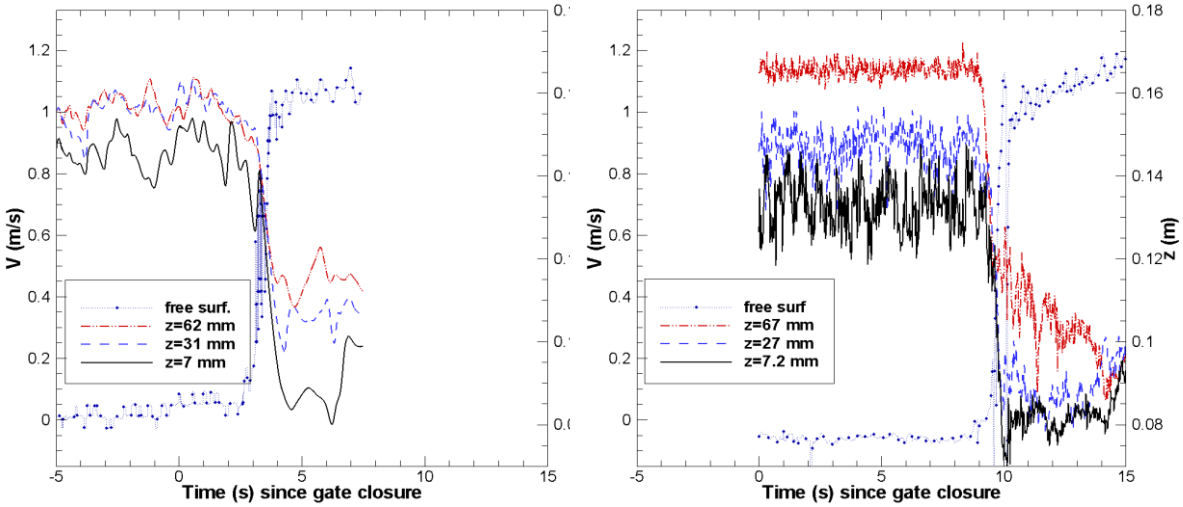

(A) Numerical data, *x=2 m* (B) Experimental data, *x=6.15 m*

Figure 3 Confrontation of longitudinal velocities recorded at different heights above the bed with the free surface evolution

In Figure 4 (A) and (B), we present the whole time evolution of the numerical streamwise velocity recorded at two vertical elevations, respectively *z=0.007 m* and *z=0.062 m* along the numerical channel. The SEM method transmits the turbulence at the inlet boundary of the channel. It took *5 s to* the turbulence to reach the outgoing boundary of the numerical channel. The velocity presents a similar pattern during the simulation and the same discrepancies with the experimental data are observed along the channel. The small flow reversal observed for *x=2 m* and *z=0.007 m* is only present at *0.2 m* from the left wall. Another interesting feature is the perturbation for the velocity recorded at *x=4 m*. The deceleration is not obvious, which is certainly a consequence of the proximity of the inflow boundary condition.

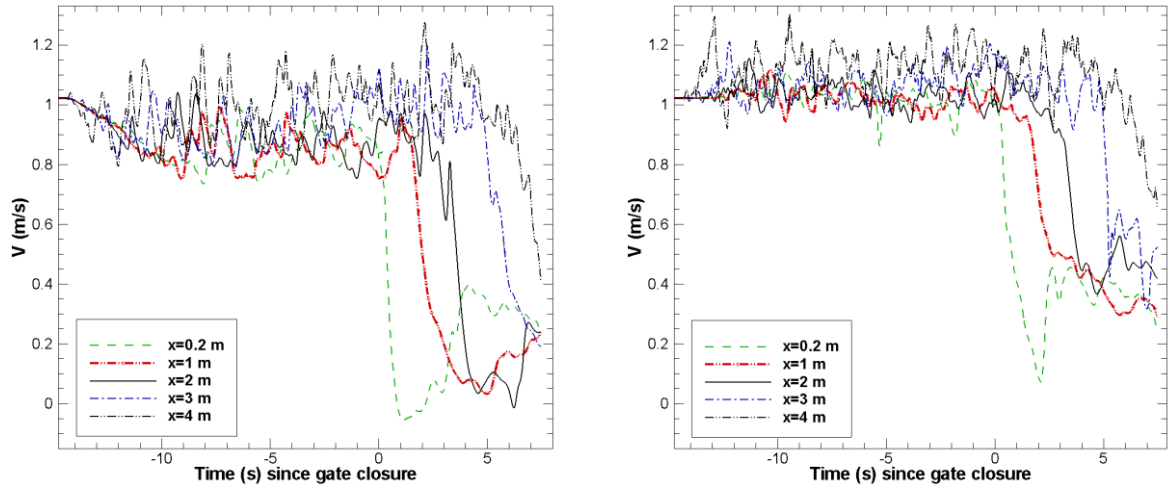

(A) Numerical data, z=0.007 m (B) Numerical data, z=0.067 m

Figure 4 Streamwise velocity recorded at different abscissae for two different elevations

Figure 5 (A) and (B) present the transverse numerical and experimental velocity signals recorded for respectively *x=2 m* and *x=6.15 m* and two different elevations above the bed with the free surface elevation. Note that the same remarks about the recorded position apply for both numerical and experimental data. We observe no matching pattern with the experimental data. The signature of the passage of the bore is blurred in the velocity signals, except from the disappearance of the small magnitude fluctuations. We also observe that, for the different heights, the numerical velocity tends to have the same fluctuation. This may be due to the coarse mesh grid distribution in the transverse direction.

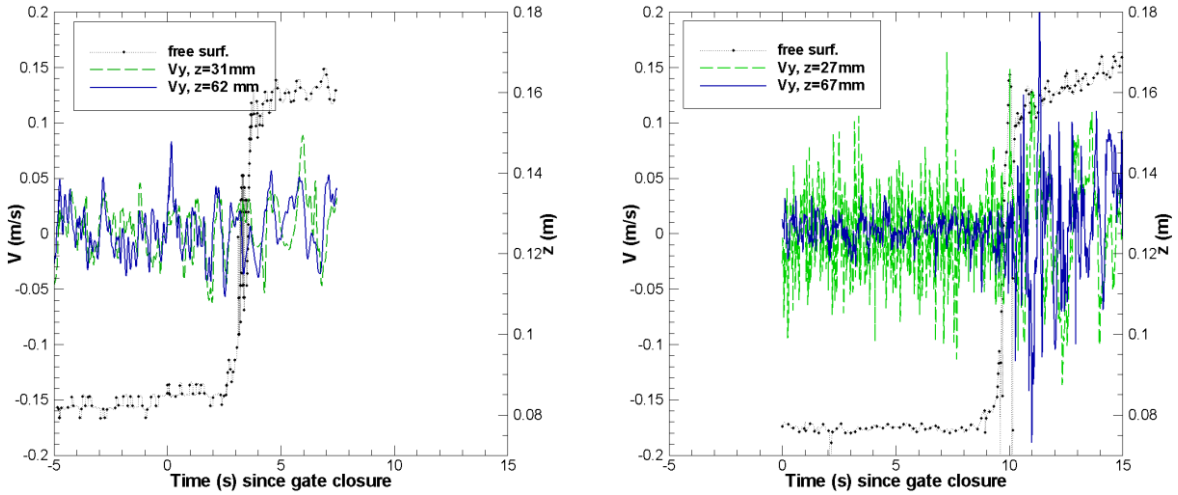

(A) Numerical data, *x=2 m* (B) Experimental data, *x=6.15 m*

Figure 5 Comparison of the transverse velocity components

4.3. Discussion

Qualitatively, the numerical results present a number of similarities with the physical study. The rapid decrease of the longitudinal velocity was observed during the bore front passage, and the same general trends were observed. The instantaneous velocity measurements and the numerical data showed a marked effect of the tidal bore front passage. Quantitatively, the free surface elevation was found to match correctly the results of Koch and Chanson (2005, 2009). The magnitude of the deceleration observed under the bore was in accord with the experimental results.

It is important to highlight that the present work has some limitations. In order to save CPU time, the numerical channel was only *5 m* long while the experimental flume was *12 m* long. As a result, the distance was too short for the inflow conditions to develop correctly. Moreover, we showed that the data obtained *1 m* after the right inflow conditions were influenced by them. The simulation had to be stopped before the bore reached the right boundary, explaining the short time for data records after the bore passage. When checking the velocity distribution as a function of the water depth, we found that the development of the boundary layer was not correctly simulated, compared to the experimental data. This might be attributed to the mesh grid refinement. On the other hand, the experimental channels were not perfectly smooth: some irregularities existed in the forms of plastics joints every *3 m* between PVC sheets and glass wall sheets. These were ignored in the numerical simulations, although the irregularities exceeded 0.5×10^{-3} *m* for bottom and lateral wall joints. Since the tidal bore is a fragile phenomenon, these irregularities might have some significant effect. In this work, the turbulence was created using the data of a single point measurement in the physical study. A better description of the physical flow will help to set up the inflow condition.

5. CONCLUSION

A Large Eddy Simulation was performed to investigate the turbulent flow motion of a breaking tidal bore with a weak breaking front in a three dimensional configuration. The numerical results were found to be encouraging. They compared well qualitatively with the experimental data, considering a first attempt to describe this complicated flow with three-dimensional numerical simulations. The discontinuity of the positive surge is described clearly. The water depth suddenly increases and the velocity under the surge decreases abruptly as documented in the study of Koch and Chanson (2009). However, the initial data before the bore were not completely satisfying as the velocity data were poorly distributed along the vertical axis.

Further three-dimensional numerical developments are under way to confirm these first observations and to investigate in more details the generation process of the recirculation structures and their three-dimensional turbulent features, as experimentally observed. The effect of the roughness of the

experimental channel will need to be carefully investigated. The numerical simulation of the total length of the experimental channel is also considered, with an appropriate mesh grid discretisation, in order to get a fully developed tidal bore to compare more clearly with the physical observations.

6. ACKNOWLEDGMENTS

The authors wish to thank the Aquitaine Regional Council for the financial support with which the TREFLE laboratory purchased a 256-processor cluster. This work was granted access to the HPC resources of CINES under the allocation 2009-c2009026104 made by GENCI (Grand Equipement National de Calcul Intensif). Prof. Hubert Chanson also acknowledges the funding for a visiting professorship position at the Université de Bordeaux, Bruno Simon acknowledges a joint scholarship funded by the TREFLE Laboratory and the Région Aquitaine; the financial assistance of the Agence Nationale de la Recherche (Projet Mascaret 10-BLAN-0911-01) is acknowledged.

7. REFERENCES

Chanson, H. (2009), *Current knowledge in hydraulic jumps and related phenomena. A survey of experimental results*. European Journal of Mechanics - B/Fluids. 28 (2), pp. 191 - 210.

Furuyama, S. and Chanson, H. (2010), *A numerical study of a tidal bore*, Coastal Engineering Journal. 52 (3), pp. 215-234.

Jarrin, N., Benhamadouche, S., Laurence, D. and Prosser, R. (2006), *A synthetic-eddy-method for generating inflow conditions for large-eddy simulations*. International Journal of Heat and Fluid Flow. 27 (4), pp. 585-593.

Koch, C. and Chanson, H. (2005), *An Experimental Study of Tidal Bores and Positive Surges: Hydrodynamics and Turbulence of the Bore Front*. The University of Queensland, Brisbane, Australia.

Koch, C. and Chanson, H. (2009), *Turbulence Measurements in Positive Surges and Bores*. Journal of Hydraulic Research, IAHR. 47 (1), pp. 29-40.

Lubin, P., Chanson, H. and Glockner, S. (2010a), *Large Eddy Simulation of turbulence generated by a weak breaking tidal bore*. Environmental Fluid Mechanics. 10 (5), pp. 587-602.

Lubin, P., Glockner, S. and Chanson, H. (2010b), *Numerical simulation of a weak breaking tidal bore*. Mechanics Research Communications. 37 (1), pp. 119-121.

Lubin, P., Vincent, S., Abadie, S. and Caltagirone, J.P. (2006), *Three-dimensional Large Eddy Simulation of air entrainment under plunging breaking waves*. Coastal Engineering. 53 (8), pp. 631-655.

Nezu, I. (2005), *Open-Channel Flow Turbulence and Its Research Prospect in the 21st Century*. Journal of Hydraulic Engineering. 131 (4), pp. 229-246.

Nezu, I. (1977), *Turbulent structures in open-channel flows*. Ph.D. Thesis Kyoto University, Japan.

Sagaut, P. (2001), *Large eddy simulations for incompressible flows: an introduction*. Springer (Scientific computation), Berlin, New York.